

Received July 13, 2019, accepted July 29, 2019, date of publication August 1, 2019, date of current version August 27, 2019.

Digital Object Identifier 10.1109/ACCESS.2019.2932419

# Acoustic Focusing Imaging Characteristics Based on Double Negative Locally Resonant Phononic Crystal

SHUAI TANG<sup>1</sup>, RUI WANG<sup>1,2</sup>, AND JIANNING HAN<sup>1,2</sup>

<sup>1</sup>School of Science, North University of China, Taiyuan 030051, China

<sup>2</sup>School of Information and Communication Engineering, North University of China, Taiyuan 030051, China

Corresponding author: Jianning Han (hanjn46@nuc.edu.cn)

This work was supported in part by the National Natural Science Foundation of China under Grant 61671414, in part by the Postdoctoral Science Foundation of China under Grant 2017M611198, in part by the Science and Technology Project of North University of China under Grant 20181546, and in part by the Science and Technology Foundation for Young Scientist of Shanxi Province, China, under Grant 201601D202035.

**ABSTRACT** To achieve high-efficiency and high-resolution acoustic focusing, we used artificial periodic acoustic structures composed of cell arrays to manipulate the acoustic transmission wave front, and used finite element software to simulate the acoustic field characteristics. We found that when focuses generated by arc-shaped acoustic excitation sources are incident on one side of the model, the energy will be localized within the structure to reduce its transmission loss, and then the high-resolution emission focus will be generated on the other side of the model. The magnitude of the acoustic pressure at the focus point will change with the frequency of the incident acoustic wave and will reach an extreme value at the resonant frequency. In addition, we explored the acoustic transmission characteristics of structures at different widths and found that it is only necessary to increase the width of the model by an integer multiple of half a wavelength to achieve low loss focusing effects at various distances. The acoustic phenomena studied in this paper may provide new methods for the application of photoacoustic signal detection, ultrasound medical imaging and ultrasonic nondestructive testing.

**INDEX TERMS** Acoustic focusing, artificial structures, local resonance.

## I. INTRODUCTION

In recent years, research on the manipulation of acoustic waves has attracted wide attention. One of the most effective ways is to design the artificial periodic structure to obtain the anomalous acoustic characteristics that traditional materials in nature do not have, such as low frequency acoustic absorption [1], [2], directional acoustic transmission [3], [4] and acoustic stealth [5]–[8].

The investigation of wave propagating in periodic media can be reduced to the solution of differential equations with periodic coefficients. One of the most popular approximations applied in this challenging field of science is the homogenization approach. [9]–[12] However, the homogenization approach does not permit stop-band effect to be determined in the first-order approximation of the averaging method.

The associate editor coordinating the review of this article and approving it for publication was Bora Onat.

In order to solve the problem, Andrianov *et al.* [13]–[15] applied the homogenization method with an asymptotic solution regarding a cell for large inclusion dimensions. The first and second approximations of the homogenization procedure can be obtained, which enables detection of the first stop-band. For validity and comparison with other approaches, they have also applied the Fourier method and found that the Fourier method was shown to work well for relatively small inclusions. These studies have provided the basis for the research of periodic structure.

As an important branch of acoustics, acoustic focusing imaging has important application value. Especially, some newly developed interdisciplinary subjects, such as photoacoustic signal detection [16]–[18], ultrasound medical imaging [19] and ultrasound non-destructive testing [20], have put forward high requirements and new challenges for high-resolution focused ultrasound imaging. In the mathematical community, there is a large recent body of work on the use of

subwavelength resonators in order to enhance the resolution. It was proved that there are two regimes: a dilute regime (volume fraction of the resonators is small) and the nondilute one, where the mechanisms of superfocusing are different. In the dilute regime, the medium behaves like a high contrast one near the resonant frequency and for some resonant structures there is a superfocusing of waves [21]–[23]. While in the nondilute regime [24], the wave has two components: a highly oscillating one multiplied by a low frequency one (which gives the envelope of the wave). These studies provide theoretical basis for the research of high-resolution lens. At the same time, a lot of novel research has emerged in lens design. In 2009, Deng *et al.* [25] used the unit cell structure with gradually changing size to achieve the focusing and amplification of parallel incident waves, which provided a direction for applications such as coupling or integration of acoustic devices. In the same year, Lin *et al.* [26] proposed a novel approach to effectively couple acoustic energy into a two-dimensional phononic-crystal waveguide by an acoustic beamwidth compressor. By gradually modulating the density and elastic modulus of the scatterers along the direction transverse to the phononic propagation, the beamwidth compressor can efficiently compress the wide acoustic beam to the scale of the phononic-crystal waveguide. In 2010, Peng *et al.* [27] used a two-dimensional sonic crystal with gradient negative refractive index to generate the focusing effect of acoustic plane waves. The gradual refractive-index was achieved by gradual modification of the lattice spacing both along the transverse and longitudinal directions. In 2016, Zhao and Wang [28] reported on the subwavelength focusing of Rayleigh waves using gradient-index (GRIN) phononic crystals made of air holes scatters in a thick silicon substrate. The subwavelength focusing was demonstrated both in the inner and in the silicon substrate behind the GRIN PCs by using a non-contact experimental technique. In the same year, Tol *et al.* [29] explored the enhancement of structure-borne elastic wave energy harvesting, both numerically and experimentally, by exploiting a Gradient-Index Phononic Crystal Lens structure. All these studies achieved the focused imaging of acoustic waves by gradually changing the structural parameters of the unit cell, such as unit size, elastic modulus and lattice constant, reflecting that the artificial periodic structure has good characteristics of acoustic wave manipulation. However, from the perspective of sample preparation, the design of the gradient structure will undoubtedly increase the difficulty of the process. Therefore, it would be of great research significance to be able to achieve high-efficiency acoustic focusing imaging characteristics using cells of the same property, size, and shape.

In this paper, based on the two-dimensional (2D) artificial unit cells of the same property, size and shape, an acoustic super-lens with a periodic structure is formed by the array. We present acoustic wave propagation from water to a periodic structure. The transmission of this coupled wave has been well studied [30]–[33]. On the basis of previous studies,

this paper explores the results by means of finite element method (FEM). Under the manipulation of the lens to the transmission wave front, the focused imaging effect of the acoustic wave can be realized, and the difficulty of sample preparation can be effectively reduced.

## II. MODEL STRUCTURE DESIGN

The acoustic model of the locally resonant periodic structure is shown in Fig. 1. It is a rectangular structure composed of an array of unit cells and placed in water. The length and width of the rectangle are 0.7 dm and 0.4 dm respectively. The unit cell is composed of two parts, one of which is a hexagonal structure surrounded by rubber balls of the same size, and the other part is a lead core wrapped by a rubber layer placed at the center of the hexagonal structure. The whole unit cell is embedded in the epoxy resin matrix. The diameter of inner lead core is 0.01 dm, the thickness of rubber coating is 0.002 dm, and the diameter of outer rubber ball is 0.01 dm. The incident acoustic wave is excited by an arc source, and the incident direction is the left side of the rectangular structure.

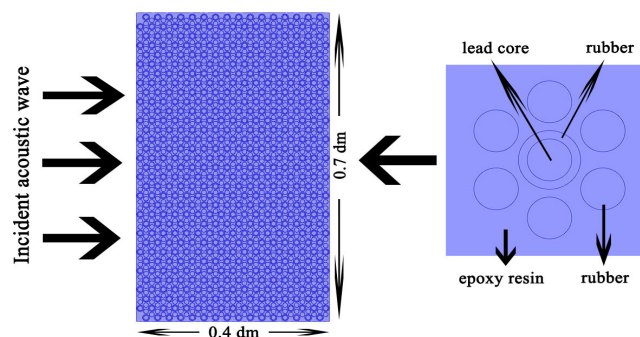


FIGURE 1. Focusing imaging model based on acoustic periodic structure.

TABLE 1. Material parameters.

Material	Density (kg/m <sup>3</sup> )	Velocity (m/s)
Water	1000	1500
Lead core	11600	2160
Rubber	980	300
Epoxy resin	1180	2680

We use COMSOL finite element software for numerical simulation, and the parameters are as shown in Table 1. First, we perform geometric modeling and material selection based on the parameters described above. Next, we choose pressure acoustics as the physical field. We use the linear elastic fluid model and the boundary of hard acoustic field (wall).

Then, we divided the grid and added the frequency domain study. Finally, the numerical simulation results are post-processed to explore the acoustic transmission characteristics of the artificial periodic structure.

### III. MODEL ANALYSIS

Similar to the optical lens imaging principle, the acoustic lens (artificial periodic structure) can manipulate the acoustic wave propagation path so that the acoustic waves passing therethrough can be focused at a certain position. In this way, imaging and recognition of the target acoustic reflection characteristics can be achieved. From the wave theory of optical and acoustic imaging, it can be known that the Fourier expansion of the wave field information of a point source placed in front of a lens includes the traveling wave component and the evanescent wave component. High-frequency components carrying subwavelength details become evanescent waves and cannot participate in imaging due to exponential attenuation of amplitude during propagation. The image produced by a common lens to a point acoustic source contains only the traveling wave component, so the imaging resolution limit of half wavelength exists in the lens imaging theory based on conventional materials. Therefore, the core of sub-wavelength imaging is to enable evanescent waves to participate in imaging, or to capture evanescent waves. The placement of an acoustic artificial periodic structure with a double negative property (negative mass and negative modulus of elasticity) in the fluid medium causes the incident acoustic wave to excite the surface wave mode at the interface of the fluid and the periodic structure, and couples the evanescent wave of the target scattering into the surface state in the near field. Through the resonance coupling, the effective transmission of the evanescent wave signal and the amplification of the amplitude can be realized, thereby realizing sub-wavelength imaging that breaks the resolution limit in the near field.

According to the foregoing, designing an acoustic lens with double negative characteristics is the key to achieving sub-wavelength acoustic signal imaging. In this paper, the negative mass density is achieved by encapsulating the soft rubber in a high-density core and embedding it in an epoxy resin. Among them, the rubber-coated lead core is heavier than the epoxy resin. As the frequency increases to near the resonant frequency, the role played by the lead core in the composite system becomes larger and larger. This inevitably causes the equivalent medium to “look” heavier and heavier until the equivalent mass density diverges at the resonant frequency. Therefore, the equivalent mass density shows a tendency to increase with frequency in a certain frequency band. In contrast, the negative elastic modulus is achieved by placing a single rubber on the epoxy resin. Since rubber is softer than epoxy resin, the role played by soft rubber in the composite system becomes more and more important as the frequency increases up to the resonant frequency. This causes the effective medium to “look” softer and softer until the

effective elastic modulus becomes negative and eventually diverges at the resonance. Therefore, near the resonant frequency, the equivalent mass density and the equivalent elastic modulus will be negative at the same time, which will lead to the realization of negative refraction effect.

As shown in Fig. 2, when the acoustic wave is incident on the negative refractive medium (artificial periodic structure) by the positive refractive medium (water), the acoustic wave will be concentrated due to the influence of the negative refractive property and a focal point will be generated at the center of the structure. This focus can be regarded as a secondary source that will continue to spread out the acoustic waves. When the acoustic wave exits the artificial periodic structure, similar to the previous process, it is affected by the negative refraction characteristics, and a focus point will be regenerated on the right side of the structure.

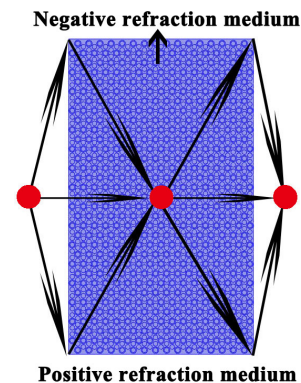


FIGURE 2. Schematic diagram of acoustic focusing.

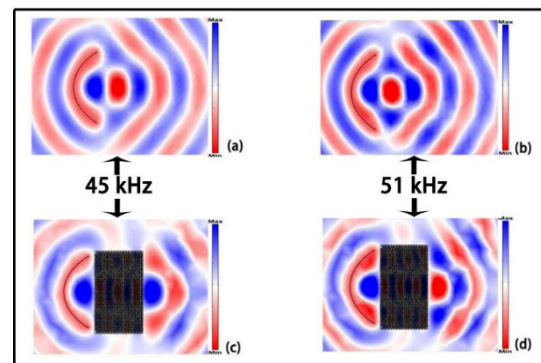
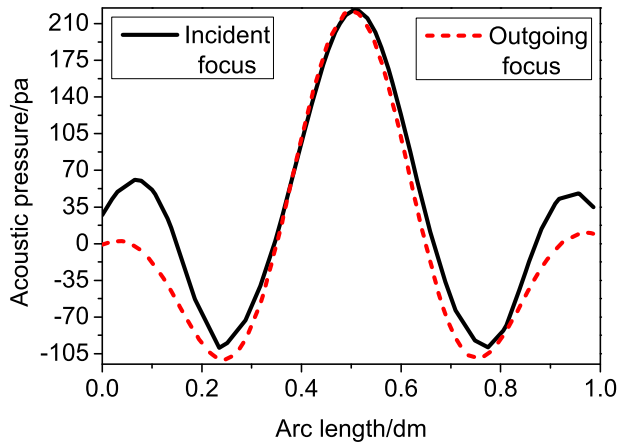


FIGURE 3. Acoustic focusing effect based on periodic structure.

### IV. RESULTS AND ANALYSIS

As shown in Fig. 3 (a) - (b), since we use an arc-shaped acoustic excitation source, the acoustic waves converge and focus on the free plane. However, the focus can only be generated near the excitation source, and will diffuse and attenuate with the increase of transmission distance. Therefore, if we want to increase the transmission distance without divergence of focus, we need to manipulate the transmission wave front,



**FIGURE 4.** The contrast curve of the acoustic pressure between the incident focus and the exit focus.

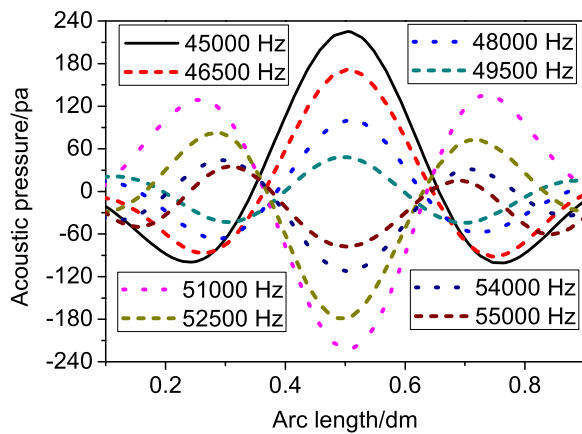


**FIGURE 5.** The relationship between the incident acoustic frequency and the outgoing acoustic pressure.

restrain its diffusion and make it converge inward. To achieve this goal, we introduce the artificial periodic structure to manipulate the acoustic wave. As shown in Fig. 3 (c) - (d), when the focus generated by the arc acoustic excitation source is incident by one side of the model, the energy is localized in the structure, transmitted through the wave front and eventually produced an emission focus on the other side of the model. Fig. 4 shows the contrast curve of the acoustic pressure between the incident focus and the exit focus. It can be found that the acoustic pressure intensity of the incident

acoustic wave does not decrease obviously after passing through the artificial acoustic structure, and the size of the emission focus is almost the same as that of the incident focus, which proves that the dispersion effect does not occur with the increase of transmission distance. Macroscopically, this achieves the low loss “removal effect” of focus.

To explore the relationship between the incident acoustic frequency and the outgoing acoustic pressure at the exit focus, as shown in Fig. 5, the frequency range of incident acoustic wave from 45000 Hz to 55000 Hz is selected and the corresponding acoustic pressure curve is made. It can be found that with the increase of frequency, the acoustic pressure amplitude first decreases and then increases. In the process of increasing from 45000 Hz to 51000 Hz, the acoustic pressure amplitude gradually decreases. But in the process of increasing from 51000 Hz to 55000 Hz, the acoustic pressure amplitude gradually increases. As two extreme points, as shown in Fig. 3 (c)-(d), 45000 Hz and 51000 Hz are respectively the incident frequency points at which the acoustic pressure amplitude reaches the positive maximum and the negative maximum. This is due to the acoustic wave produces a locally resonant effect with the periodic structure at these two incident frequencies, so that its amplitude reaches an extreme value. It is noteworthy that the “positive pressure” and “negative pressure” at the focusing point in Fig. 5 refer to the same and opposite phases of the incident acoustic wave. Since the wavelengths of different incident frequencies are different (the wavelength will decrease as the frequency increases), the focusing point in the same or opposite phase with the incident acoustic wave will appear when the structure size is fixed. The process in which the amplitude of the acoustic pressure changes from the extreme value at the same phase to the opposite phase as the frequency changes can be regarded as a vibration period. Therefore, the acoustic wave can focus at multiple incident frequencies, and the closer it approaches the resonance frequency in a certain vibration period, the higher the acoustic pressure amplitude of the focus.

Fig. 6 shows height expression of acoustic pressure at different frequencies, in which the length and width of the periodic structure remain fixed, 0.7 dm and 0.4 dm, respectively. It can be found that the incident acoustic wave propagates through one wave front, two wave fronts and three wave fronts at resonance frequencies of 33000 Hz, 45000 Hz

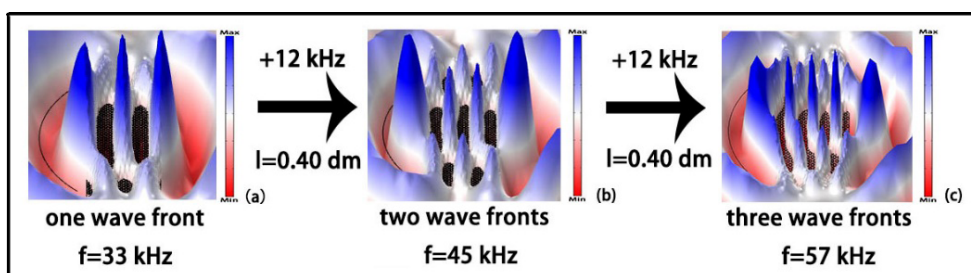


**FIGURE 6.** The height expression of acoustic pressure at different frequencies.

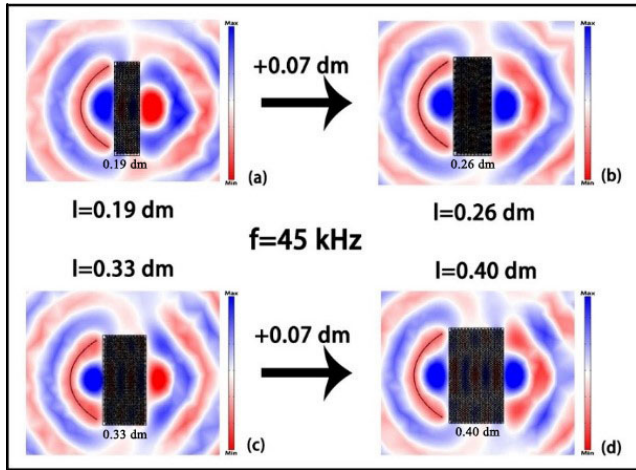


FIGURE 7. Acoustic field distribution of structures with different widths.

and 57000 Hz, respectively, and the focus imaging point can be realized on the other side of the structure. It can be inferred that 12000 Hz is the frequency domain range of each vibration period. Therefore, in the passband of the artificial periodic structure, the locally resonant focusing can be realized in the next vibration period as long as the resonance frequency of the artificial periodic structure is increased at 12000 Hz as the step length. In addition, to explore the influence of model width on the transmission characteristics of acoustic waves, as shown in Fig. 7, we have made acoustic field distributions under different structure widths at the same incident frequency (45 kHz). When the width increases from

0.19 dm to 0.40 dm with the step size of 0.07 dm, the focus of the outgoing acoustic wave alternates with the positive and negative phases of the incident acoustic wave. Where 0.07 dm is the distance of half wavelength. Therefore, as long as the width of the periodic structure is increased by an integer multiple of half wavelength, the transmission distance of acoustic wave can be manipulated.

### V. EXPERIMENTAL TEST

In this section, we designed an experimental test system. The flow chart of the system is shown in Figure.8. Here, an amplifier circuit was used to enhance the weak ultrasonic signal to obtain the analog voltage required by the subsequent analog-to-digital converter. To achieve a gain of greater than 80 dB, we used an AD603 chip (Tsinghua Unisplendour, China) to design the amplifier circuit.

The artificial periodic structure proposed in this paper is a 3D layered structure. As shown in Fig. 9, we use laser engraving technology to make samples. We incident the focused acoustic wave from the center position on the left side of the sample, and placed an acoustic detection array on the right side of the sample. The array consists of nine probes in the same row, each of which is 30 mm apart. Waveforms of the detected data are shown in Fig.10. Therefore, as shown in Fig.11, we plot the acoustic pressure distribution curve according to the acoustic pressure amplitude at different positions. The acoustic pressure clearly approaches zero at the 120-mm position. At 0 mm, which is the center of the other side of the model, a clear focusing phenomenon can be seen.

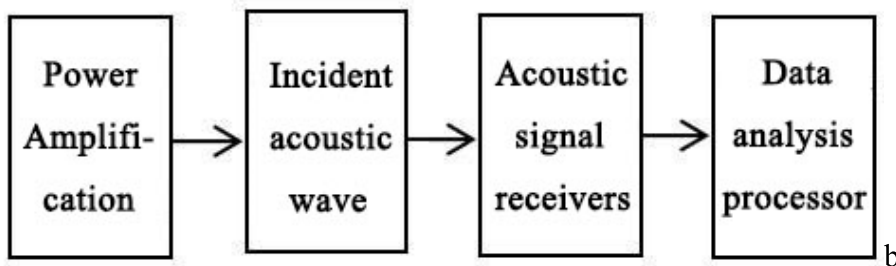


FIGURE 8. Design of test system.

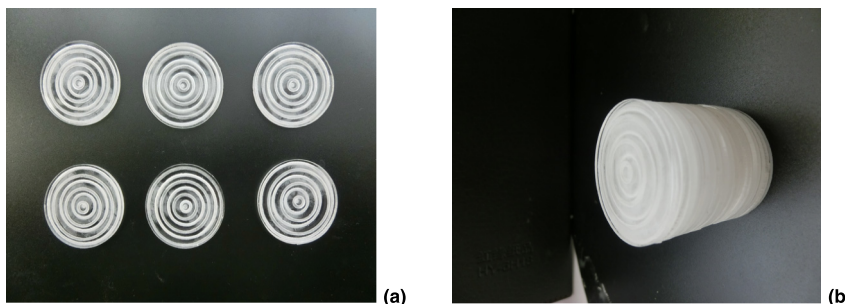


FIGURE 9. Experimental samples based on laser engraving technology. (a) Single-layer structure; (b) Multilayer structure.

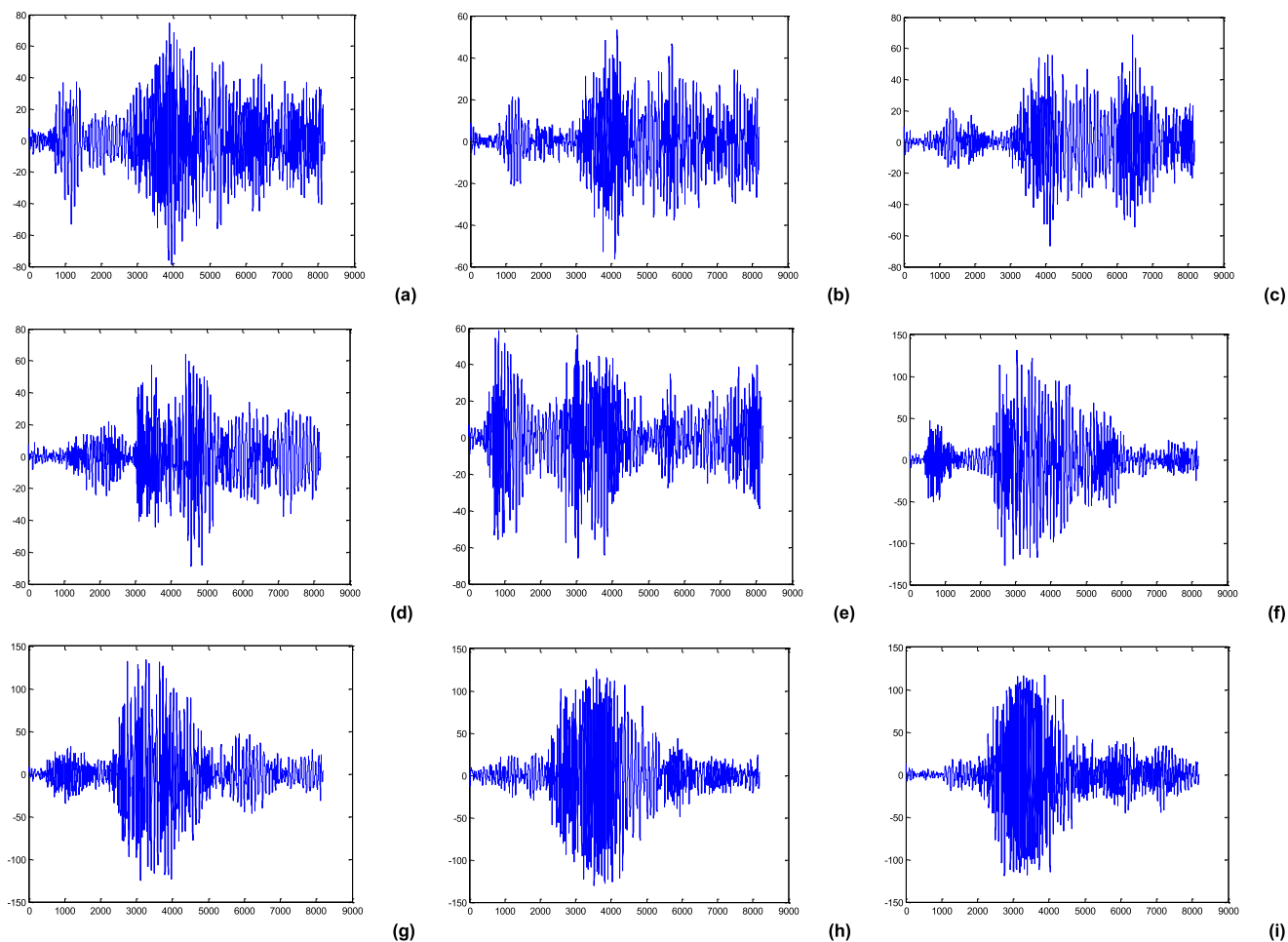


FIGURE 10. Waveforms of test data: (a) +30 mm; (b) +60 mm; (c) +90 mm; (d) +120 mm; (e) 0 mm; (f) -30 mm; (g) -60 mm; (h) -90 mm; (i) -120 mm.

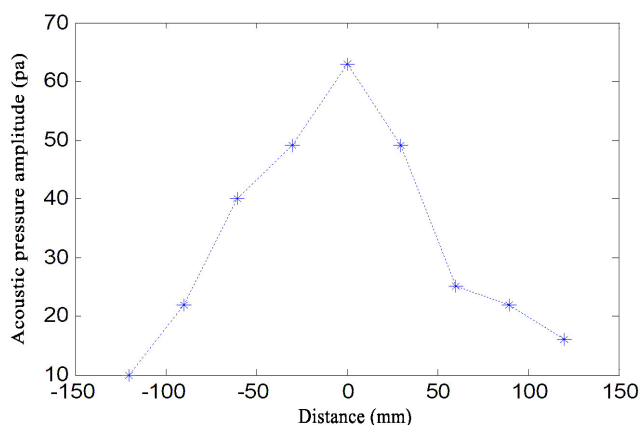


FIGURE 11. Acoustic field distribution.

### VI. CONCLUSION

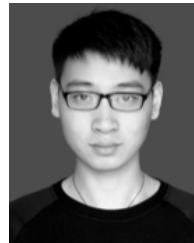
In this paper, the artificial periodic structure was designed based on the unit cell, and the acoustic field characteristics of the structure were simulated by finite element software. The artificial manipulation of the acoustic transmission wave front was realized. The results showed that when the focus

generated by the arc-shaped acoustic excitation source is incident on one side of the model, the energy will be localized inside the structure to reduce its transmission loss, and then the high-resolution focus will be generated on the other side of the model. From the macro point of view, this realizes the low loss “removal effect” of focus. In addition, artificial periodic structure has many vibration periods. The magnitude of acoustic pressure at the focus will change with the frequency of incident acoustic wave, and will reach the maximum at the resonance frequency of each period. According to the transmission characteristics of the structure at different widths, we also found that it is only necessary to increase the width of the model by an integer multiple of half a wavelength to achieve low loss focusing effects at various distances. Our research may provide new methods for the application of photoacoustic signal detection, ultrasound medical imaging and ultrasonic nondestructive testing.

### REFERENCES

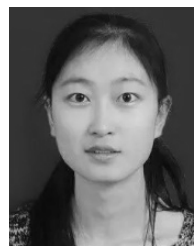
[1] N. Gao, Z. Wei, H. Hou, and A. O. Krushynska, “Design and experimental investigation of V-folded beams with acoustic black hole indentations,” *J. Acoust. Soc. Amer.*, vol. 145, Jan. 2019, Art. no. EL79.

- [2] N. Gao, J. H. Wu, H. Hou, and L. Yu, "Excellent low-frequency sound absorption of radial membrane acoustic metamaterial," *Int. J. Mod. Phys. B*, vol. 31, no. 3, 2017, Art. no. 1750011.
- [3] S.-D. Zhao, Y.-S. Wang, and C. Zhang, "High-transmission acoustic self-focusing and directional cloaking in a graded perforated metal slab," *Sci. Rep.*, vol. 7, no. 1, 2017, Art. no. 4368.
- [4] L. Fan, H. Ge, S.-Y. Zhang, H.-F. Gao, Y.-H. Liu, and H. Zhang, "Nonlinear acoustic fields in acoustic metamaterial based on a cylindrical pipe with periodically arranged side holes," *J. Acoust. Soc. Amer.*, vol. 133, no. 6, p. 3846, 2013.
- [5] H. Chen and C. T. Chan, "Acoustic cloaking in three dimensions using acoustic metamaterials," *Appl. Phys. Lett.*, vol. 91, no. 18, 2007, Art. no. 183518.
- [6] S. Zhang, C. Xia, and N. Fang, "Broadband acoustic cloak for ultrasound waves," *Phys. Rev. Lett.*, vol. 106, no. 2, 2011, Art. no. 024301.
- [7] M. Farhat, S. Enoch, S. Guenneau, and A. B. Movchan, "Broadband cylindrical acoustic cloak for linear surface waves in a fluid," *Phys. Rev. Lett.*, vol. 101, no. 13, 2008, Art. no. 134501.
- [8] H. Shen, M. P. Păidoussis, J. Wen, D. Yu, L. Cai, and X. Wen, "Acoustic cloak/anti-cloak device with realizable passive/active metamaterials," *J. Phys. D: Appl. Phys.*, vol. 45, no. 28, pp. 1–7, 2012.
- [9] N. S. Bakhvalov and G. Panasenko, *Homogenisation: Averaging Processes in Periodic Media: Mathematical Problems in the Mechanics of Composite Materials*. Dordrecht, The Netherlands: Kluwer, 1989.
- [10] A. Bensoussan, G. C. Papanicolaou, and J.-L. Lions, *Asymptotic Analysis for Periodic Structures*. Amsterdam, The Netherlands: North-Holland, 1978.
- [11] N. S. Bakhvalov and M. E. Eglit, "Long-wave asymptotics with dispersion for waves propagation in stratified media, I. Waves orthogonal to the layers," *Russian J. Numer. Anal. Math. Model.*, vol. 15, no. 1, pp. 3–14, 2000.
- [12] N. S. Bakhvalov and M. E. Eglit, "Long-wave asymptotics with dispersion for waves propagation in stratified media, II. Waves in an arbitrary direction," *Russian J. Numer. Anal. Math. Model.*, vol. 15, nos. 3–4, pp. 225–236, 2000.
- [13] I. V. Andrianov, J. Awrejcewicz, V. V. Danishevskiy, and D. Weichert, "Wave propagation in periodic composites: Higher-order asymptotic analysis versus plane-wave expansions method," *J. Comput. Nonlinear Dyn.*, vol. 6, no. 1, pp. 011015-1–011015-8, 2010.
- [14] I. V. Andrianov, V. I. Bolshakov, V. V. Danishevskiy, and D. Weichert, "Higher order asymptotic homogenization and wave propagation in periodic composite materials," *Proc. Roy. Soc. A, Math., Phys. Eng. Sci.*, vol. 464, no. 2093, pp. 1181–1201, 2008.
- [15] B. S. M. E. Hai and M. Bause, "Finite element approximation of wave propagation in composite material with asymptotic homogenization," in *Proc. ASME Turbo Expo, Turbine Tech. Conf. Expo.*, Düsseldorf, Germany, vol. 7A, Jun. 2014, Art. no. V07AT28A009.
- [16] L. Dhar and J. A. Rogers, "High frequency one-dimensional phononic crystal characterized with a picosecond transient grating photoacoustic technique," *Appl. Phys. Lett.*, vol. 77, no. 9, pp. 1402–1404, 2000.
- [17] B. Wu and G. J. Diebold, "Photoacoustic effect in a sinusoidally modulated structure," *Appl. Phys. Lett.*, vol. 100, no. 16, 2012, Art. no. 164102.
- [18] M. P. Mienkina, C.-S. Friedrich, N. C. Gerhardt, M. F. Beckmann, M. F. Schiffner, M. R. Hofmann, and G. Schmitz, "Multispectral photoacoustic coded excitation imaging using unipolar orthogonal Golay codes," *Opt. Express*, vol. 18, no. 9, pp. 9076–9087, 2010.
- [19] A. M. Deylami and B. M. Asl, "A fast and robust beamspace adaptive beamformer for medical ultrasound imaging," *IEEE Trans. Ultrason., Ferroelectr., Freq. Control*, vol. 64, no. 6, pp. 947–958, Jun. 2017.
- [20] T. Kim, J. Kim, and X. Jiang, "AIN ultrasound sensor for photoacoustic Lamb wave detection in a high temperature environment," *IEEE Trans. Ultrason., Ferroelectr., Freq. Control*, vol. 65, no. 8, pp. 1444–1451, Aug. 2018.
- [21] H. Ammari, B. Fitzpatrick, D. Gontier, H. Lee, and H. Zhang, "Sub-wavelength focusing of acoustic waves in bubbly media," *Proc. Roy. Soc. A, Math., Phys. Eng. Sci.*, vol. 473, no. 2208, 2017, Art. no. 20170469.
- [22] H. Ammari and H. Zhang, "Super-resolution in high-contrast media," *Proc. Roy. Soc. A, Math. Phys. Eng. Sci.*, vol. 471, Jun. 2015, Art. no. 20140946.
- [23] H. Ammari and H. Zhang, "Effective medium theory for acoustic waves in bubbly fluids near minnaert resonant frequency," *SIAM J. Math. Anal.*, vol. 49, no. 4, pp. 3252–3276, 2017.
- [24] H. Ammari, H. Lee, and H. Zhang, "Bloch waves in bubbly crystal near the first band gap: A high-frequency homogenization approach," *SIAM J. Math. Anal.*, vol. 51, no. 1, pp. 45–59, 2017.
- [25] K. Deng, Y. Ding, Z. He, H. Zhao, J. Shi, and Z. Liu, "Theoretical study of subwavelength imaging by acoustic metamaterial slabs," *J. Appl. Phys.*, vol. 105, no. 12, 2009, Art. no. 124909.
- [26] S.-C. S. Lin, B. R. Tittmann, J.-H. Sun, T.-T. Wu, and T. J. Huang, "Acoustic beamwidth compressor using gradient-index phononic crystals," *J. Phys. D: Appl. Phys.*, vol. 42, no. 18, 2009, Art. no. 185502.
- [27] S. Peng, Z. He, H. Jia, A. Zhang, C. Qiu, M. Ke, and Z. Liu, "Acoustic far-field focusing effect for two-dimensional graded negative refractive-index sonic crystals," *Appl. Phys. Lett.*, vol. 96, no. 26, 2010, Art. no. 263502.
- [28] S.-D. Zhao and Y.-S. Wang, "Negative refraction and imaging of acoustic waves in a two-dimensional square chiral lattice structure," *Comptes Rendus Physique*, vol. 17, no. 5, pp. 533–542, 2016.
- [29] S. Tol, F. L. Degertekin, and A. Erturk, "Gradient-index phononic crystal lens-based enhancement of elastic wave energy harvesting," *Appl. Phys. Lett.*, vol. 109, no. 6, 2016, Art. no. 063902.
- [30] S. Mönkölä, "Numerical simulation of fluid-structure interaction between acoustic and elastic waves," Ph.D. dissertation, Jyväskylä Univ., Jyväskylä, Finland, 2011.
- [31] B. S. M. E. Hai and M. Bause, "Numerical study and comparison of alternative time discretization schemes for an ultrasonic guided wave propagation problem coupled with fluid-structure interaction," *Comput. Math. Appl.*, to be published. doi: 10.1016/j.camwa.2019.01.009.
- [32] B. S. M. E. Hai and M. Bause, "Finite element approximation of fluid-structure interaction with coupled wave propagation," *Proc. Appl. Math. Mech.*, vol. 17, no. 1, pp. 511–512, 2018.
- [33] B. S. M. E. Hai, M. Bause, and P. Kuberry, "Modeling and simulation of ultrasonic guided waves propagation in the fluid-structure domain by a monolithic approach," *J. Fluids Struct.*, vol. 88, pp. 100–121, Jul. 2019.



**SHUAI TANG** was born in Xuzhou, Jiangsu, China, in 1995. He received the B.S. degree in communication engineering from the North University of China, Taiyuan, in 2017, where he is currently pursuing the M.S. degree in physics.

His research interest includes acoustic metamaterials.



**RUI WANG** was born in Taiyuan, Shanxi, China, in 1994. She received the B.S. degree in applied mathematics from Lvliang University, Lvliang, in 2017. She is currently pursuing the M.S. degree in mathematics with the North University of China, Taiyuan, China.

Her research interest includes acoustic metamaterials.



**JIANNING HAN** was born in Taiyuan, Shanxi, China, in 1980. He received the B.Sc. degree in electronic information engineering and the M.Sc. degree from the North University of China, China, where he is currently a Lecturer with the School of Information and Communication Engineering. He has teaching experience of 11 years. He has published over seven papers in various journals. His research interests include acoustic signal processing and graphics processing. He has completed five scientific research projects.

• • •